Cell. Mol. Life Sci. (2012) 69:1377–1389
DOI 10.1007/s00018-011-0884-2

Cellular and Molecular Life Sciences

RESEARCH ARTICLE

Tbx2 and Tbx3 induce atrioventricular myocardial development and endocardial cushion formation

Reena Singh · Willem M. Hoogaars · Phil Barnett · Thomas Grieskamp · M. Sameer Rana · Henk Buermans · Henner F. Farin · Marianne Petry · Todd Heallen · James F. Martin · Antoon F. M. Moorman · Peter A. C. 't Hoen · Andreas Kispert · Vincent M. Christoffels

Received: 20 September 2011 / Revised: 25 October 2011 / Accepted: 7 November 2011 / Published online: 1 December 2011

Abstract A key step in heart development is the coordinated development of the atrioventricular canal (AVC), the constriction between the atria and ventricles that electrically and physically separates the chambers, and the development of the atrioventricular valves that ensure unidirectional blood flow. Using knock-out and inducible overexpression mouse models, we provide evidence that the developmentally important T-box factors Tbx2 and Tbx3, in a functionally redundant manner, maintain the AVC myocardium phenotype during the process of chamber differentiation. Expression profiling and ChIP-sequencing analysis of Tbx3 revealed that it directly interacts with and represses chamber myocardial genes, and induces the atrioventricular pacemaker-like phenotype by activating relevant genes. Moreover, mutant mice lacking 3 or 4 functional alleles of *Tbx2* and *Tbx3* failed to form atrioventricular cushions, precursors of the valves and septa. Tbx2 and Tbx3 trigger development of the cushions through a regulatory feed-forward loop with Bmp2, thus providing a mechanism for the co-localization and coordination of these important processes in heart development.

Keywords Endocardial cushion · Mesenchyme · Atrioventricular · T-box factors · Tbx3 · BMP · Differentiation · Interaction · Repression

R. Singh, W. M. Hoogaars and P. Barnett contributed equally to this work.

A. Kispert and V.M. Christoffels contributed equally as the senior authors of this work.

Electronic supplementary material The online version of this article (doi:10.1007/s00018-011-0884-2) contains supplementary material, which is available to authorized users.

R. Singh · T. Grieskamp · H. F. Farin · M. Petry · A. Kispert (✉)
Institut für Molekularbiologie, Medizinische Hochschule Hannover, 30625 Hannover, Germany
e-mail: kispert.andreas@mh-hannover.de

W. M. Hoogaars · P. Barnett · M. S. Rana · A. F. M. Moorman · V. M. Christoffels (✉)
Heart Failure Research Center, Academic Medical Center, University of Amsterdam, 1105 AZ Amsterdam, The Netherlands
e-mail: v.m.christoffels@amc.uva.nl

H. Buermans · P. A. C. 't Hoen
Department of Human Genetics, Leiden University Medical Center, Leiden, The Netherlands

T. Heallen · J. F. Martin
Texas A&M Health Science Center, Institute of Biosciences and Technology, Houston, TX, USA

Introduction

Atria and ventricles arise in a highly localized fashion from an initially linear tube in the embryonic heart. These embryonic chambers feature an increased cell proliferation and a working type of myocardial gene program. They are initially separated by the atrioventricular canal (AVC) that by virtue of its lower cell division rate provides a primitive morphological constriction. Because the myocardial lining of the AVC remains of a primitive type with low conductivity [1], it will delay the propagation of the electrical impulse between atria and ventricles. Most of the myocardial investment of the AVC will have disappeared by the end of gestation, but some nodal type of cells remain and form the AV junction and AV node, and continue to relay the impulse to the ventricles. Furthermore, the AV myocardium induces the overlying endocardium to

undergo an epithelial–mesenchymal transition (EMT) and to invade the cardiac jelly, an extracellular matrix (ECM) that is deposited by the primary myocardium. These mesenchymal cushions are subsequently remodeled into thin valve leaflets, AV insulation, and components of the septa that ensure structural and functional compartmentalization of the heart [2–4].

Given the common developmental origin of AV nodal cells, insulation and valves, it may not be surprising that patients with congenital AVC defects often suffer from additional conduction problems, and that patients with Ebstein's anomaly, where the tricuspid valve is incorrectly positioned and hypomorphic, frequently display ventricular pre-excitation [5]. These observations indicate a common regulatory pathway for the formation of the AVC/conduction system and the mesenchymal components of valves and septa.

BMP signaling plays a critical role in both AVC specification and the formation of cushion tissue [4]. Myocardial bone morphogenetic protein 2 (*Bmp2*) activates myocardial expression of the transcriptional repressor *T-box 2* (*Tbx2*), and is thought to directly induce cushion formation in the adjacent endocardium [2, 3, 6–9]. Additionally, *Tbx2* inhibits the chamber myocardial gene program in the AVC [10–12]. *Tbx3* is genetically and functionally related to *Tbx2*, and suppresses chamber differentiation of the sinus node, the AV bundle and bundle branches [13, 14]. *Tbx2* and *Tbx3* expression overlaps in the AVC, suggesting that functional redundancy has prevented a full appreciation of their role in the development of this tissue to date [12]. Here, we present data in the mouse that implicate a feed-forward loop between *Tbx2*/*Tbx3* and *Bmp2* in this tissue.

Materials and methods

Mice and genotyping

Mouse work was performed in accordance with national and international guidelines

Mice carrying a null allele of *Tbx2* ($Tbx2^{tm1.1(cre)Vmc}$, synonyms: $Tbx2^{-}$, $Tbx2^{Cre}$) [10] and/or *Tbx3* ($Tbx3^{tm1.1(cre)Vmc}$, synonyms: $Tbx3^{-}$, $Tbx3^{Cre}$) [13] and mice for Cre-mediated misexpression of *Tbx2* or *Tbx3*, *NppaCre* [15], *Myh6Cre* [16], *Myh6-MerCreMer* [17] and *CAG-CAT-TBX3* (*CT3*) [13], and $Nkx2\text{-}5^{Cre/+}$ and $Bmp2^{floxneo/-}$ [3] were previously described. For conditional misexpression of *Tbx2*, a *Tbx2* expression cassette was introduced in the *Hprt* locus (*HpCT2*) (see online data supplement). All strains were maintained on outbred (NMRI or FVB/N) background.

Generation of the $Hprt^{TBX2}$ allele

A 'knock-in' strategy into the X-chromosomal *hypoxanthine guanine phosphoribosyl transferase* (*Hprt*) gene locus was designed to replace mayor parts of the *Hprt* exon 1 (including the ATG) by a cassette suited for cre-mediated (mis-) expression described previously [18]. Homologous recombination results in a functional *Hprt* null allele, allowing direct selection of successfully targeted ES cells by 6-Thioguanine. The targeting vectors contained a 2.2-kbp 5′-homology region, followed by the ubiquitously expressed CMV early enhancer/chicken β-actin (CAG) promoter, the conditional expression cassette [18], and a 5.1-kbp 3′-homology region. The open reading frame (ORF) of human *TBX2* (cDNA NM_005994.3) [19] was first subcloned in the vector *pSL1180* (GE-healthcare), 5′ of an *IRES-EGFP* sequence, and then shuttled as 5′-*NheI-ORF-IRES-EGFP-MluI*-3′ fragment into the *Mlu*I and *Nhe*I sites of the targeting vector. This results in a reverse orientation of the ORF, relative to the CAG promoter, avoiding 'leaky' expression. After cre-mediated 'flipping'- and excision events between pairs of *loxP* and *loxM* sequences, the ORF locates in sense direction, directly downstream of the CAG promoter. The targeting vector was verified by sequencing before linearization and electroporation in *Hprt*-positive SV129 ES cells (maintained beforehand in HAT medium). A two-step selection protocol was employed, starting 24 h after electroporation with the addition of 100 µg/ml G418, followed by the addition of 1.67 µg/ml 6-Thioguanine (Sigma) after an additional 5 days. Surviving colonies were expanded and genotyped by PCR (conditions are available upon request). To test the functionality of the expression cassette in candidate ES clones, the GFP epifluorescence was analyzed 6 days after electroporation with a cre-expression plasmid (*pCAG::turbo-cre,* kind gift from Achim Gossler). Verified ES clones were microinjected into CD1 mouse blastocysts. Chimeric males were obtained and mated to NMRI females to produce heterozygous F1 females.

Generation and isolation of transgenic embryos/mice

For the generation of *Tbx2* or *Tbx3* mutant embryos, mice heterozygous for *Tbx2* or *Tbx3* null alleles were intercrossed. For the generation of double-mutant embryos, double-heterozygous mice were intercrossed. Double-transgenic mice conditionally expressing *TBX3* in the atria and the whole heart were generated by crossing *CT3* mice with *NppaCre* or *Myh6Cre* mice, respectively. Double-transgenic mice conditionally expressing *Tbx2* in the whole heart were generated by crossing *HpCT2* mice with *Myh6Cre* or $Mox2^{Cre}$ mice. For timed pregnancies, vaginal plugs were checked in the morning after mating, noon was

taken as embryonic day (*E*) 0.5. Embryos were harvested in PBS, fixed in 4% paraformaldehyde overnight and stored in 100% methanol at −20°C before further use. Wild-type littermates were used as controls. Genomic DNA prepared from yolk sacs or tail biopsies was used for genotyping by PCR (see supplementary table 6).

Embryonic heart explant assay

Atria from *Myh6-Cre;HpCT2* and control (*Myh6-Cre*) E10.5 embryos were dissected, individually placed on Transwell filters and cultured for 4 days in presence or absence of 30 μM Dorsomorphin in explant medium (Optimem supplemented with Penicillin/Streptomycin, Glutamax, FCS (2%), Insuline/Transferrin/Selenium). Total RNA was extracted with RNAPure reagent (Peqlab) and DNaseI (Roche) treated for 30 min at 37°C. RNA was reverse transcribed with RevertAid H-minus M-MuLV reverse transcriptase (Fermentas). For semi-quantitative PCR, the number of cycles was adjusted to the mid-logarithmic phase. Quantification was performed with Quantity One software (Bio-Rad). Normalization was against Gapdh. Assays were performed at least twice in duplicates. *P* values were calculated using the unpaired two-tailed Student's *t* test. See supplementary table 6 for primer sequences and PCR conditions.

Sample preparation, RNA isolation, and gene expression analysis

Left atria of six *NppaCre;CT3* mice and six control (*NppaCre*) mice (male, 6 weeks) were dissected and snap frozen in liquid nitrogen. Total RNA was isolated and purified using single prep nucleospin columns according to the manufacturer's instructions (Macherey–Nagel). RNA quality was checked using a bioanalyzer (Agilent Technologies). A total of 250 ng of total RNA was used for biotin-16-UTP cRNA labeling and amplification using the Illumina RNA amplification kit (Ambion Inc., Austin, TX). Labeled RNA was hybridized to Illumina MouseRef-6 BeadChip following the manufacturer's instructions (Illumina Inc., San Diego, CA). The arrays were scanned using an Illumina Bead array reader confocal scanner. BeadStudio software was used to assess the individual array quality. Unprocessed intensity values were averaged per bead type, exported from BeadStudio and subsequently normalized using VSN in *R* [20]. Genes were tested for significant differential expression using the empirical Bayes moderated *t*-statistics test in the R-Limma package [21] at a 5% Benjamini–Hochberg false discovery rate [22]. We found that the expression of 737 transcripts was significantly reduced in atria of *NppaCre;CT3* mice, whereas 809 transcripts were significantly induced (threshold: p value <0.05).

Geneset analysis and GO term selection

The Global test [23] was used to test for significant association of specific GO terms with the differences in phenotypes between the *NppaCre;CT3* and *NppaCre* mice. A series of selection criteria was applied to reduce the list of significant GO terms, i.e., Benjamini–Yekutieli FDR at 15% and the number of genes in the geneset between 10 and 75. The individual influence of each gene on the test statistics was calculated and used as an additional level of GO term selection, i.e., at least five genes per geneset with an influence above 5, representing at least 5% of the geneset.

Quantitative real-time PCR analysis

Quantitative real-time PCR analysis was performed as described previously [13]. In short, total RNA was isolated from left atrial appendices of 4-week-old adult mice using the RNeasy mini kit according to the manufacturer's protocol (Qiagen). cDNA was reverse transcribed from 300 ng total RNA using the superscript II system (Invitrogen) and expression of different genes was assayed with quantitative real-time PCR using the Roche 480 Lightcycler. Relative start concentration ($N_{(0)}$) was calculated as described previously [24]. Values were normalized to *Gapdh* expression levels. Primers sequences are provided in the online supplemental table 6.

In situ hybridization and immunohistochemistry

Non-radioactive in situ hybridization was performed as described previously [25]. Probes for *Bmp10*, *Sox9, Fbln2*, and *Id3* were kindly provided by Herman Neuhaus, Benoit de Crombrugghe and Yvette Chin. IMAGE cDNA constructs were kindly provided by Fred van Ruissen. The following IMAGE cDNA constructs were digested with *SalI* and labeled with T7 RNA polymerase to generate DIG-labeled probes used for in situ hybridization: *Tagln* (BC003795), *Fbln2* (BC005443), *Lum* (BC005550), *Nkd2* (BC019952), *Meox1* (BC011082), *Ednra* (BC008277), and *Aldh1b1* (BC020001). *Fgf12, Cacna2d2*, and *Hnt* probe construct were generated by PCR amplification using gene-specific primers and were subsequently cloned into *pBluescript SK* vector for DIG labeling. For immunohistochemistry, the same fixation protocol as for the in situ hybridization analysis was used. Primary antibodies used were as follows: anti-cleaved caspase 3 (Cell Signaling, #9661 polyclonal) and anti-phosphohistone H3 (Cell Signaling, #9701 polyclonal).

ChIP data analysis

Conditional TBX3 over-expressing and cardiac specific tamoxifen inducible Cre (Mer-Cre-Mer) mice have been

described before [13, 17]. Male mouse hearts were isolated 4 days after intra-peritoneal injections of tamoxifen, and TBX3 over-expression was confirmed by qRT-PCR, in situ hybridization and immunohistochemistry (not shown). ChIP was performed on mouse hearts using anti-TBX3 (A-20, Santa-Cruz). In this case, Mer-Cre-Mer mice, lacking the *TBX3* expression construct, injected with tamoxifen served as ChIP control. Isolated DNA fragments were analyzed using high-throughput sequencing (data and analysis will be published elsewhere). Data significance of TBX3 binding peaks were analyzed using Fisher's exact test with comparison to ChIP control data.

Transcription factor binding site prediction

To identify potential T-box binding sites, high-quality position weight matrices from Jaspar database were used (http://jaspar.genereg.net/; MA0009.1 for T-box binding sites). The relative score threshold was set to 70%.

Results

Tbx2 and *Tbx3* are redundantly required for AVC patterning

Previous analyses indicated that *Tbx2* is necessary and sufficient to suppress chamber gene expression in the AVC [10, 11, 26]. However, in our *Tbx2* loss-of-function mouse AVC formation at E9.5 was grossly normal, and *natriuretic peptide type A* (*Nppa/ANF*) and other chamber markers were not ectopically expressed in the AVC [10]. *Tbx2* is co-expressed in the AVC myocardium with the closely related family member *Tbx3* arguing for functional redundancy of the two genes in this region. We wished to test this hypothesis by generating mice double mutant for *Tbx2* and *Tbx3*. This effort was largely hampered by the fact that mice double heterozygous for *Tbx2* and *Tbx3* null alleles with a high penetrance exhibited postnatal lethality due to craniofacial defects [27]. Nonetheless, we managed to obtain some double-heterozygous animals for further interbreeding. Viable $Tbx2^{-/-};Tbx3^{-/-}$ embryos from few litters at E9.5 appeared slightly retarded in their development, most likely due to arising hemodynamic failure. Morphologically, the constriction between the left ventricle and the atrium was largely absent (Fig. 1). Markers of chamber myocardium [*Nppa*, *gap junction protein, alpha 5* (*Gja5/Cx40*)] [26] were expanded into this region whereas homozygous mutants for either *Tbx2* or *Tbx3* and double heterozygous mutants showed proper chamber gene repression in the AVC (Fig. 1; data not shown). *Cre* from the mutant alleles reflecting endogenous expression from either *Tbx2* or *Tbx3* or both in the absence of Tbx2 or Tbx3 protein, was present, although reduced in $Tbx2^{-/-};Tbx3^{-/-}$ embryos (Fig. 1, arrows), indicating that early AVC specification had occurred.

A Bmp2-Tbx2/3 feed-forward loop is required for EMT and formation of cushion mesenchyme in the AVC

Histological analysis of embryos compound mutant for null alleles of *Tbx2* and *Tbx3* revealed that loss of more than two functional alleles resulted in reduction of cardiac jelly and absence of AV cushion formation (Fig. 2). *Bmp2* expression in the AVC myocardium is both required and sufficient to induce cushion formation and EMT of the adjacent endocardium [2, 3, 6]. Both *Tbx2* and *Tbx3* were downregulated in $Nkx2\text{-}5^{Cre};Bmp2^{floxneo/floxneo}$ embryos, in which *Bmp2* was inactivated in the heart (Fig. 3a), suggesting that the two genes are downstream mediators of *Bmp* signaling in this region. Expression of *Bmp2* was normal in single mutants but reduced in compound mutants indicating the presence of a feed-forward loop between Bmp2 and Tbx2/Tbx3 (Fig. 3b). Consistently, expression of transforming growth factor, beta 2 (*Tgfb2*), a Bmp2 target in this tissue that is required for cushion formation and of hyaluronan synthase 2 (*Has2*), required for cardiac jelly formation and AV cushion development [2, 28] was downregulated in the AVC endocardium and myocardium of both $Nkx2\text{–}5^{Cre};Bmp2^{floxneo/floxneo}$ embryos and compound *Tbx2/3* mutants (Online Fig. 1). Hence, *Tbx2* and *Tbx3* are required in a redundant fashion to maintain the primary myocardium of the AVC, to maintain *Bmp2* expression, and to induce the formation of cushion tissue from the endocardium in this region.

Myocardial *Tbx2* and *Tbx3* induce mesenchymal cushion formation

To further elucidate the role of Tbx2 and Tbx3 in AVC and cushion development we used gain-of-function approaches to ectopically express *Tbx2* and *Tbx3* during early heart development. We crossed mice that harbored a Cre-activatable *Tbx2* expression cassette in the transcriptionally competent *Hprt* locus (*HpCT2*) with *Myh6Cre* mice (Fig. 4a). Double-heterozygous *Myh6Cre;HpCT2* embryos survived until E13.5–E14.5. Widespread activation of *Tbx2* in the myocardium of the embryonic heart occurred relatively late at low levels, explaining the formation of chambers and the lack of early lethality observed previously using a constitutive over-expression approach [26]. Histological and in situ hybridization analyses revealed that ectopically expressed Tbx2 suppressed the expression of chamber markers *Gja5* and *Nppa* at E11.5 as expected (Fig. 4b and not shown). Formation of ectopic subendocardial mesenchyme was observed in the atria, and to

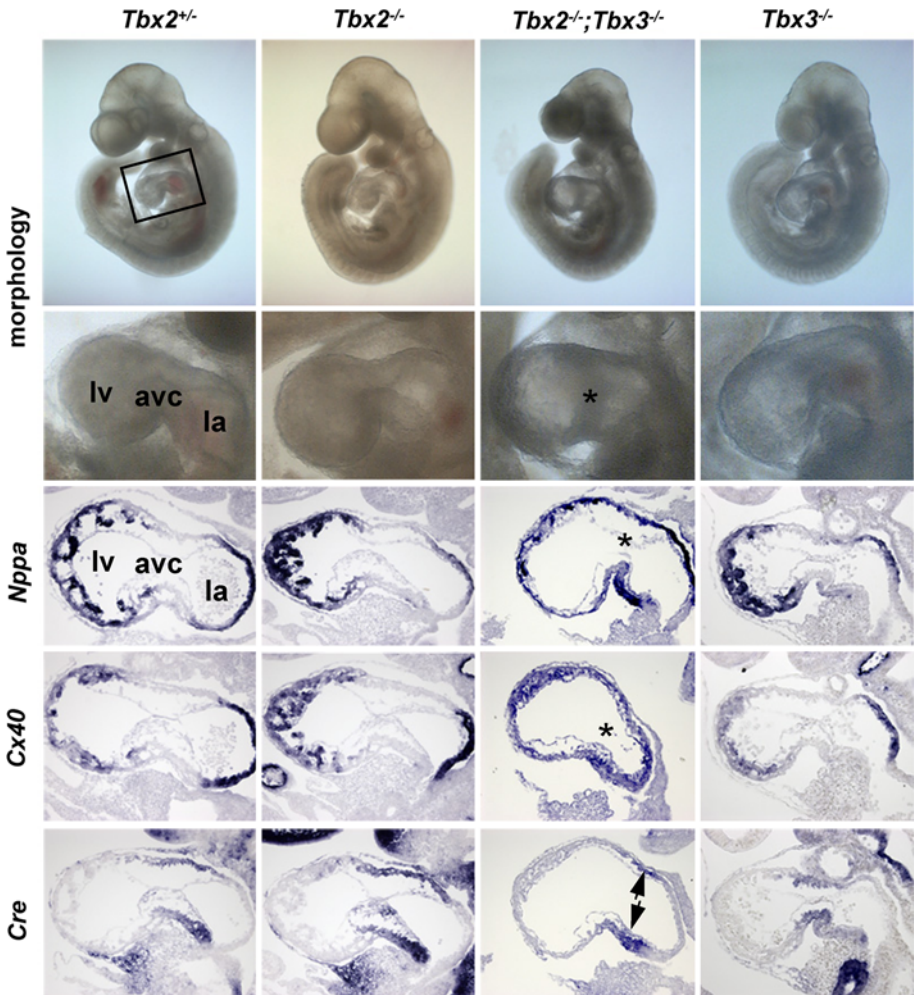

Fig. 1 Combined loss of *Tbx2* and *Tbx3* abrogates myocardial patterning of the atrioventricular canal. Comparative analysis of wild-type, $Tbx2^{-/-}$, $Tbx2^{-/-};Tbx3^{-/-}$ and $Tbx3^{-/-}$ embryos for cardiac morphology and molecular marker expression at E9.5. Left lateral views of whole E9.5 embryos and enlarged hearts (*boxed* regions in *upper row* shown in *second row*) reveal growth retardation and dilated avc phenotype in *Tbx2/Tbx3* double mutant embryos. In situ hybridization analysis of marker gene expression in sagittal sections through the avc with probes as indicated. *avc* atrioventricular canal, *la* left atrium, *lv* left ventricle

a lesser extent in the ventricles, which might be less susceptible to signals initiating cushion formation. *Bmp2* was strongly induced in the atrial myocardium, whereas Notch gene homolog 1 (*Notch1*), a Bmp2 target which regulates EMT in the endocardium [2, 4], and *Has2,* were induced in the endocardium overlying the transgenic $Tbx2^{+}$ myocardium (Fig. 4b).

We next wished to test whether induction of endocardial cushion formation by Tbx2 depends on Bmp2 signaling. For this purpose, we cultured explanted E10.5 *Myh6-Cre;HpCT2* atria for 4 days in the absence or presence of 30 μM Dorsomorphin, an inhibitor of Bmp type 1 receptors. qRT-PCR assays revealed that all markers for EMT and cushion formation tested were down-regulated in the presence of Dorsomorphin (Online Fig. 2), providing further evidence that Tbx2-mediated EMT and cushion formation depends on Bmp-signaling.

To investigate whether Tbx3 is also sufficient to induce cushion formation, we ectopically activated *Tbx3* expression in the developing heart using the *Myh6Cre* line and the Cre-activatable transgenic *Tbx3* cassette reported on earlier *CAG-CAT-TBX3* (*CT3*) [13] (Fig. 4c). Loss of *Gja5* and *Bmp10* expression confirmed functional TBX3 overexpression in double heterozygous (*Myh6Cre;CT3)* mice. *Myh6Cre;CT3* embryos featured hypoplastic chamber walls, and the fraction of phospho-Histone 3-positive proliferating cells in the ventricular walls was reduced (Fig. 4d). In contrast, ectopic *TBX3* expression did not result in induced apoptosis as defined by TUNEL assays (not shown). These results suggest that Tbx3 contributes to the low proliferation of the AVC myocardium. *Bmp2* was ectopically activated in the myocardium of *Myh6Cre;CT3* embryos, whereas snail homolog 1 (*Snai1*), a Notch1/Tgfb2 target required for AVC EMT[4] and *Has2* were ectopically activated in the overlying endocardium (Fig. 4e). Moreover, a large subendocardial space formed that, closer to the AV cushions, was filled with mesenchymal cells expressing the cushion marker *MAD homolog 6* (*Smad6*) (* in Fig. 4e; Online Fig. 3).

We next assessed the consequences of prolonged cardiac expression of *Tbx3* using *NppaCre* to activate *Tbx3* from E10 onwards in the atrial myocardium in the *CT3* mice (Fig. 5a) [13]. E17.5 fetuses formed a thick sub-endocardial layer of cells in the atria. This tissue expressed

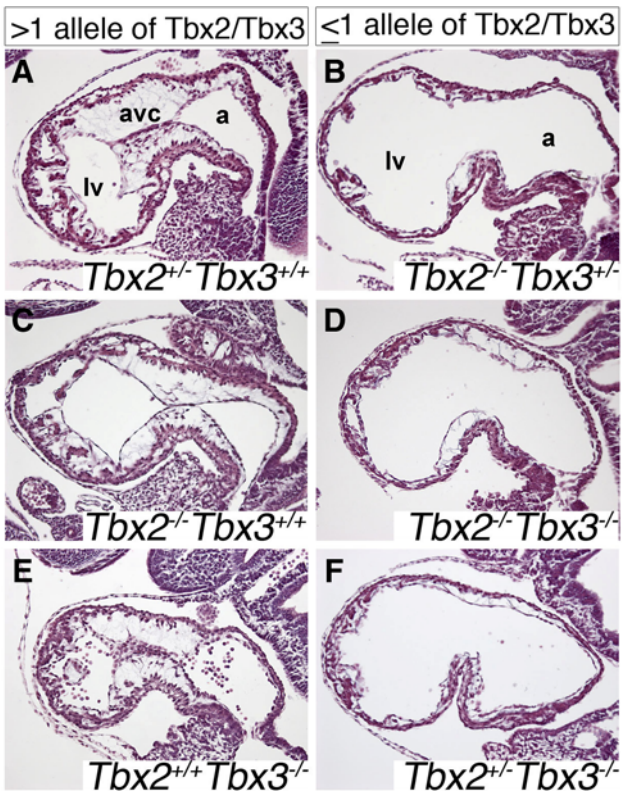

Fig. 2 Combined loss of more than two alleles of *Tbx2* and *Tbx3* abrogates cushion formation in the AVC. Histological analysis of sagittal sections through the left atrium (*la*), atrioventricular canal (*avc*), and left ventricle (*lv*) by hematoxylin and eosin (*H* and *E*) staining shows normal cushion formation upon loss of one or two functional alleles of *Tbx2* and *Tbx3* (**a**, **c**, **e**), whereas loss of more than two functional alleles of the two genes results in partial loss of cardiac jelly and complete loss of AV cushion tissue (**b**, **d**, **f**). *avc* atrioventricular canal, *a* atrium, *lv* left ventricle

mesenchymal marker genes including *actin, alpha 2, smooth muscle, aorta* (*Acta2/α-SMA*), *fibulin 2* (*Fbln2*), *versican* (*Cspg2/Vcan*) and *lumican* (*Lum*) (Fig. 5b–d, Supplemental Table 1) that are associated with AV cushions. Furthermore, *Tgfb2, Bmp6, inhibitor of DNA binding 3* (*Id3*) and *SMAD family member 6* (*Smad6*) were induced in the endocardial layers (Fig. 5c, Supplemental Fig. 4, Supplemental Table 1). Taken together, both Tbx2 and Tbx3 in myocardium are sufficient to induce cushion formation and EMT in the adjacent endocardium.

Identification of endocardial mesenchyme gene programs downstream of myocardial Tbx3

We used the *NppaCre;CT3* transgenic model to gain deeper insight into the mechanism of gene regulation by Tbx3. Genome-wide microarray analyses (Illumina MouseRef-6 oligonucleotide BeadChips, 47,769 different oligonucleotides) were performed, comparing the atrial gene expression profile of six male double-transgenic *NppaCre;CT3* mice and six male *NppaCre* control mice. Expression of 737 transcripts was significantly reduced in atria of *NppaCre;CT3* mice, whereas 809 transcripts were significantly induced (threshold: p value <0.05). Components of the Tgfβ-, Bmp-, Fgf- and Wnt-signaling pathways that have been functionally implicated in AV cushion and valve formation [2] were highly up-regulated in atria of *NppaCre;CT3* compared to *NppaCre* control mice (Supplemental Table 1). Furthermore, GO terms associated with EMT, such as TGF-β receptor signaling pathway, collagen and ECM were over represented in genes with overall higher expression in atria of *NppaCre;CT3* (Supplemental Table 2). In addition, qRT-PCR and in situ hybridization analysis confirmed expression of genes in the subendocardial mesenchyme of *NppaCre;CT3* mice (*Twist1*, *Msx1*, *Meox1*, *Sox9, Id3*, and *Smad6)* (Fig. 5d, Supplemental Fig. 4, Supplemental Table 1), whose expression and functional relevance in EMT and cushion formation in the AVC have been reported [2–4]. Furthermore, expression of *Fgfr2*, and of Wnt antagonists *Frzb*, *Sfrp2* and *Nkd2* was detected in the cushion mesenchyme and up-regulated in atria of *NppaCre;CT3* mice, compatible with the established requirement for Fgf- and Wnt-signaling in cushion and valve formation (Fig. 5d, Supplemental Fig. 5, Supplemental Table 1) [2]. *Pkd2* is normally expressed in the developing valves and was induced in atrial mesenchyme of *NppaCre;CT3* mice (Fig. 5d). In human and mouse, mutations of *Pkd2* result in valve abnormalities [29]. An additional 47 induced genes were identified in the microarray data whose specific expression in the fetal AV valvular mesenchyme was reported by Genepaint (http://www.genepaint.org/) (Supplemental Table 3). Furthermore, we provide a list of genes associated with cushion formation and EMT, as generated with the literature-base gene annotation tool Anni 2.0 [30] in Supplemental Table 4. This list contains established (e.g. *Tgfb2*, *Gata4*) as well as potential new players in cardiac cushion formation/EMT. Gli pathogenesis related protein-2 (*Glipr-2)*, for instance, has been shown to be up-regulated during tissue fibrosis, a common pathway in the progression of many chronic disease states, and have the capacity to induce EMT in renal epithelial cells [31]. Further, both *Tnc* (Tenascin-C), *Timp1* (Tissue inhibitor of matrix metalloproteinase 1) and *Hgf* have been linked to EMT via their involvement in the remodeling processes of the extracellular matrix and effects on cell motility during cellular migration [31–33].

Tbx3 imposes a nodal gene program on atrial myocardium

We observed down-regulation of known and novel chamber-specific genes in *Tbx3*-expressing atria of *NppaCre;CT3* mice (Supplemental Table 1). qRT-PCR and in situ

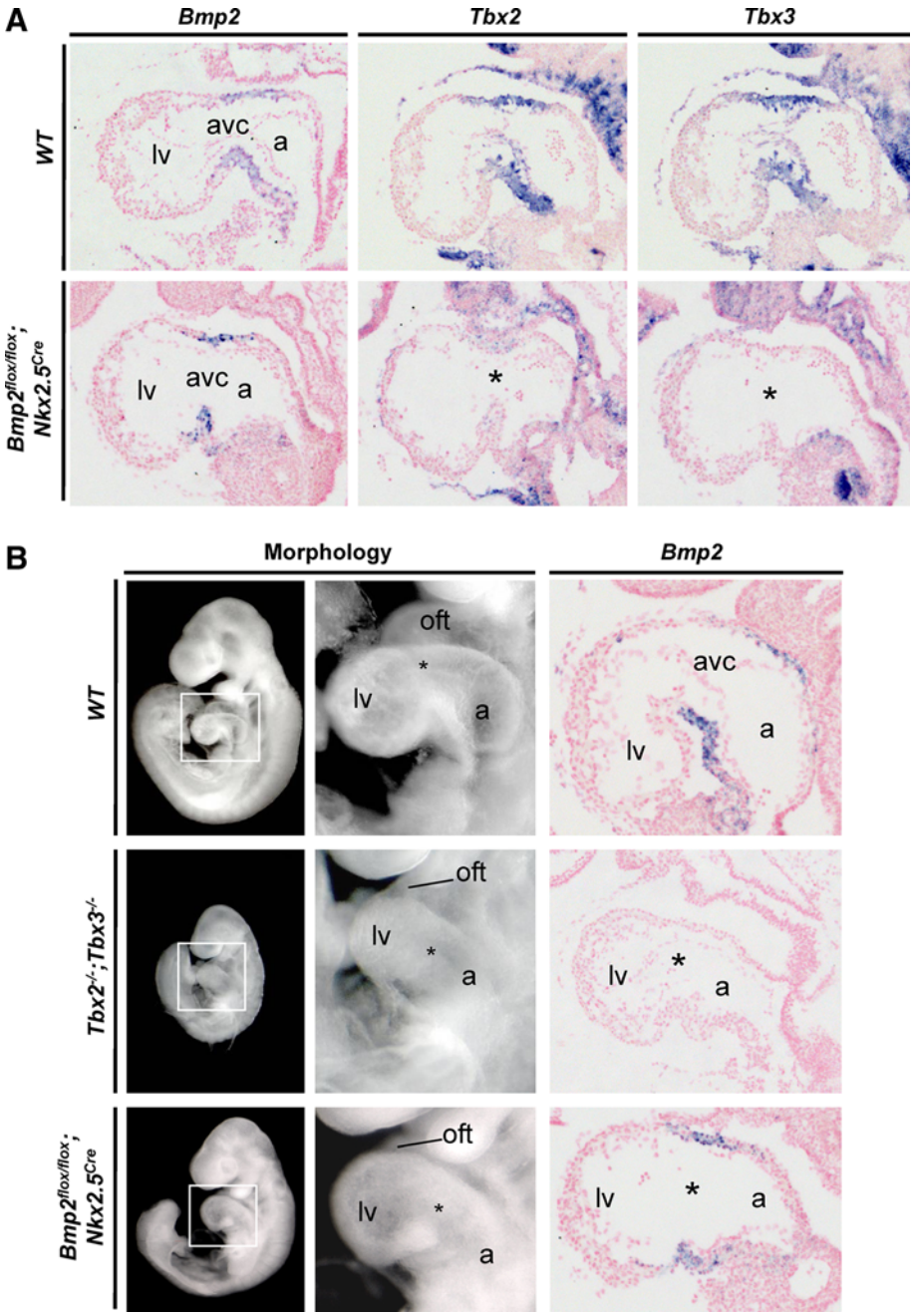

Fig. 3 A Bmp2-Tbx2/3 regulatory feed-forward loop for expression in the atrioventricular canal. **a** Inactivation of *Bmp2* in cardioblasts or embryonic cardiomyocytes by *Nkx2–5*^{Cre} results in loss of *Tbx2* and *Tbx3* expression in the atrioventricular canal (*asterisk*). **b** In both compound *Tbx2/Tbx3* mutants and *Bmp2* conditional mutants, the atrioventricular constriction is largely absent. *Bmp2* expression is lost from *Tbx2/Tbx3* compound mutants, whereas reduced levels of *Bmp2* transcripts (lacking exon 3; [3]) can still be found in the *Bmp2* conditional mutants (*asterisk*). *avc* atrioventricular canal, *a* atrium, *lv* left ventricle

hybridization analysis confirmed normal chamber-restricted expression and TBX3-mediated atrial repression of *Ckm* [34], *Nppb* [35], *Aldh1b1* and *Ednra* [36], and of *Bmp10* [37] (Fig. 5d, Supplemental Fig. 4, 5). Furthermore, atria of *NppaCre;CT3* mice had reduced expression of genes involved in muscle contractility, such as sarcomere complex genes and genes associated with mitochondria and their energy metabolism (Online Table 1). Consistently, compared to working myocytes, nodal (conduction system) myocytes feature a much poorer myofibril differentiation and sparser mitochondria [1].

Microarray analysis and subsequent validation by qRT-PCR and/or in situ hybridization revealed induction of genes in *NppaCre;CT3* atria including *Bmp2*, *Cx45/Gja7, Itpr1, Slco3A1, Id2, Cacna2d2,* and *Hnt* (Fig. 5b–d, Supplemental Fig. 5, Supplemental Table 1), normally enriched in conduction system components, including the AV node. These genes are associated with (*Slco3A1*) or involved in the formation (*Id2, Bmp2*) or function (*Cx45*, *Itpr1*) of the conduction system [1, 3, 38–40]. Regulatory sequences of the *Slco3A1* gene are thought to drive reporter gene expression of the cardiac conduction system reporter

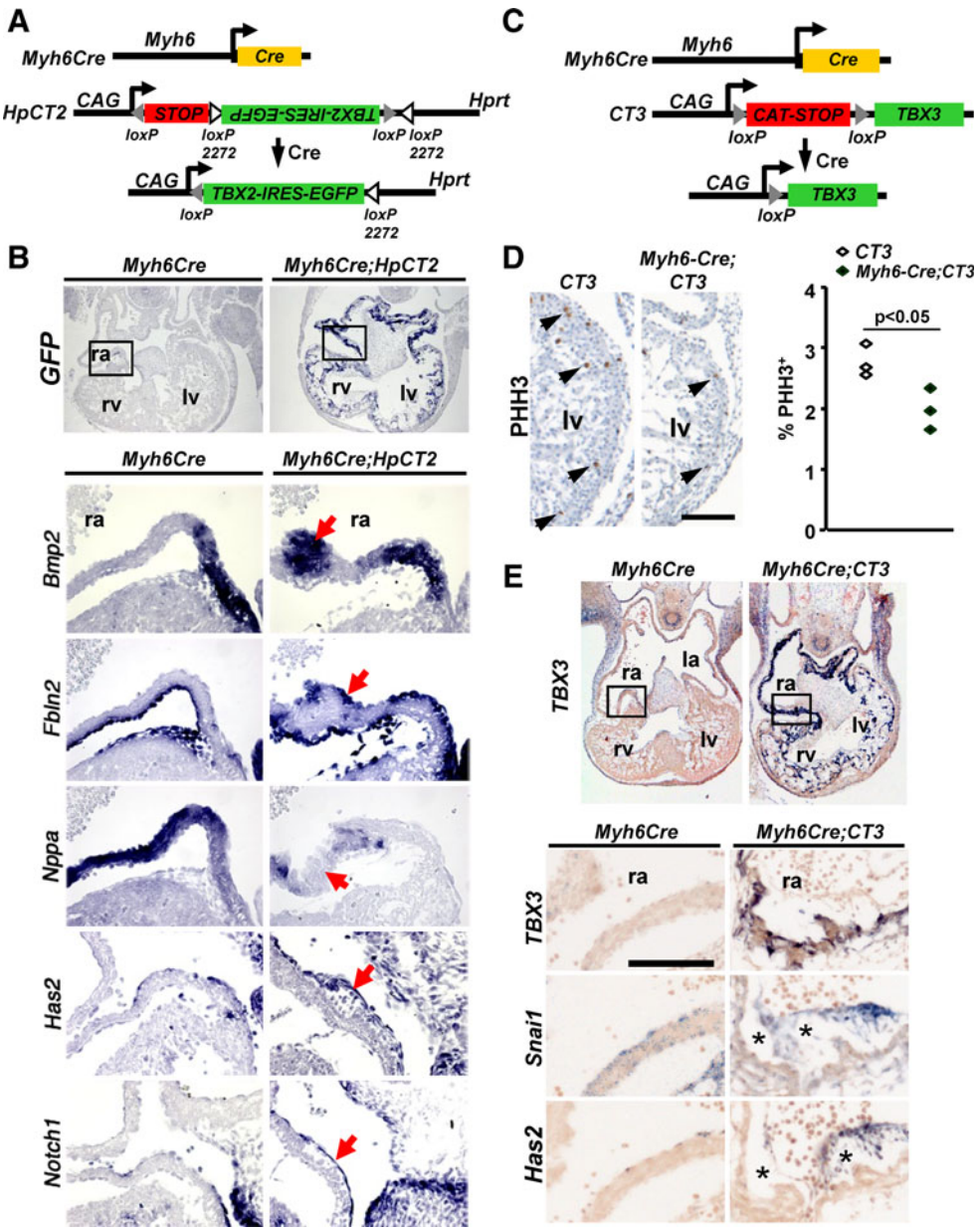

Fig. 4 Cardiac misexpression of *Tbx2* or *Tbx3* induces cardiac jelly and cushion formation in chamber myocardium. **a** Use of *Myh6Cre* driver to ectopically activate *Tbx2* in the myocardium. **b** Robust activation of *Tbx2* (*Gfp*) in *Myh6Cre;HpCT2* leads to loss of *Nppa* and induction of *Bmp2* in the myocardium, and *Fbln2, Has2* and *Notch1* in endocardium/mesenchyme (*red arrows*). **c** Transgenic constructs used to activate *Tbx3* in the myocardium of the embryonic heart. **d** Immunohistochemical analysis of proliferation (PHH3) in E11.5 hearts of *Myh6Cre;CT3* mice compared to control (*CT3*) mice. *Black arrows* depict Phospho-H3 positive cells in the ventricular myocardium of control mice and *Myh6Cre;CT3* mice. *Black bar*, 100 µm. **e** In situ hybridization of serial sections in E11.5 hearts of *Myh6Cre;CT3* mice compared to control mice. *Snai1* and *Has2* are induced in the endocardium and subendocardial mesenchyme formed in the atria of *Myh6Cre;CT3* embryos (*asterisk*). *avc* atrioventricular canal, *l/ra* left/right atrium, *l/rv* left/right ventricle

(CCS)-*lacZ* mouse strain [39]. Calcium channel subunit *Cacna2d2* and *Hnt*, which are enriched in the sinus and AV node of adult mice [41] and in the developing cardiac conduction system, including the AVC (Online Fig. 5), were strongly induced in the atria of *NppaCre;CT3* mice (Fig. 5, Supplemental Table 1).

We complemented the microarray analysis by performing ChIP-seq assays on hearts of mice in which Tbx3 was activated in the myocardium using tamoxifen-induced Cre recombination (due to technical limitations we were not able to obtain ChIP-seq data for endogenous Tbx3 from embryonic hearts). We observed several thousand peaks in the genome of *Myh6-MerCreMer;CT3* mice, whereas tamoxifen-treated *Myh6-MerCreMer* mice did not yield specifically localized peaks. Interaction with T-box binding elements (TBEs) previously identified by mutational and in vitro binding analyses (*Nppa, Myh6, Gjd3/Cx30.2, Id2*) [38, 42–45], confirms the quality of the ChIP-seq data, and implies that Tbx3 directly regulates these genes in vivo (Fig. 6a, b, Supplemental Fig. 6). Moreover, binding of Tbx5 and Gata4, derived from recently published resource of ChIP-seq data from the heart derived cell line HL-1 (GEO: GSE21529) [46] coincided with Tbx3 peaks found in these loci (Fig. 6a, b). Analysis of the overlap between the microarray and the Tbx3 ChIP-seq data sets (online supplemental table 5) revealed a significant enrichment of Tbx3 binding peaks associated with both up- and down-regulated genes. Furthermore, down-regulated genes were associated with significantly more Tbx3 binding peaks than up-regulated genes, in keeping with the notion that Tbx3

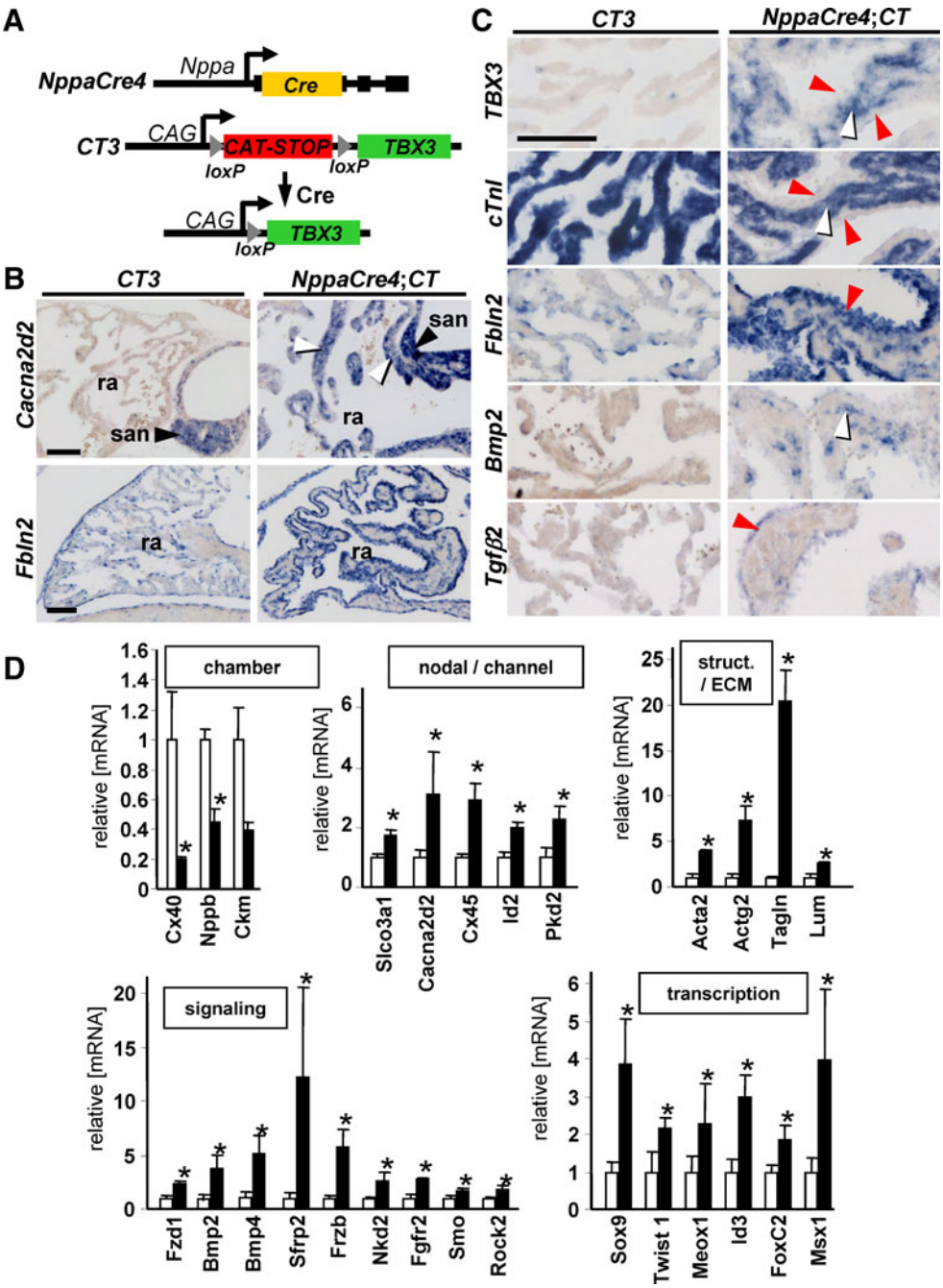

Fig. 5 Myocardial Tbx3 expression induces endocardial mesenchyme formation and nodal gene expression. **a** Transgenic constructs used to activate *TBX3* in the developing atria. **b**, **c** Sections of E17.5 atria of *CT3* and *NppaCre;CT3* mice were probed for expression of indicated genes. *Black arrowhead* indicates the sinus node (san), *white arrowhead* the myocardium. *Red arrowheads* depict the thick endocardial mesenchymal layer that forms in *NppaCre;CT3* atria. *Black bar*, 100 µm. **d** qRT-PCR analysis of left atria of *NppaCre;CT3* double-transgenic mice compared to *CT3* control mice. Expression levels in *CT3* atria were set to 1. $*p < 0.05$. *ra* right atrium, *san* sinus node

acts as a strong transcriptional repressor in vitro and in cell culture. Overlap of the Tbx3-enriched datasets with the Tbx5 ChIP-seq data obtained in HL1 cardiac-like cells revealed an average association of 90% of these enriched genes with Tbx5 [46]. The observed interaction with the region of *Nppb*, *Hcn4, Acta2, Cacna2d2, Bmp2* and *Bmp4* suggests that T-box factors also directly regulate these genes (Fig. 6b, c; Online Fig. 7). Two genes that are not influenced by Tbx3 in the myocardium but indirectly in the endocardium, *Has2* and *Sox9*, were indeed devoid of any Tbx3 peaks (Online Fig. 7).

Closer inspection of the *Bmp2* locus revealed one particular genomic site with which Tbx3 interacts (Fig. 6c). In the developing heart, enhancer associated co-factor *p*300 was also found to interact with this region (Fig. 6c) [47]. When isolated and tested in transfection assays, this fragment stimulated reporter gene expression in cardiac-like H10 cells and responded to T-box factors (Fig. 6d). These

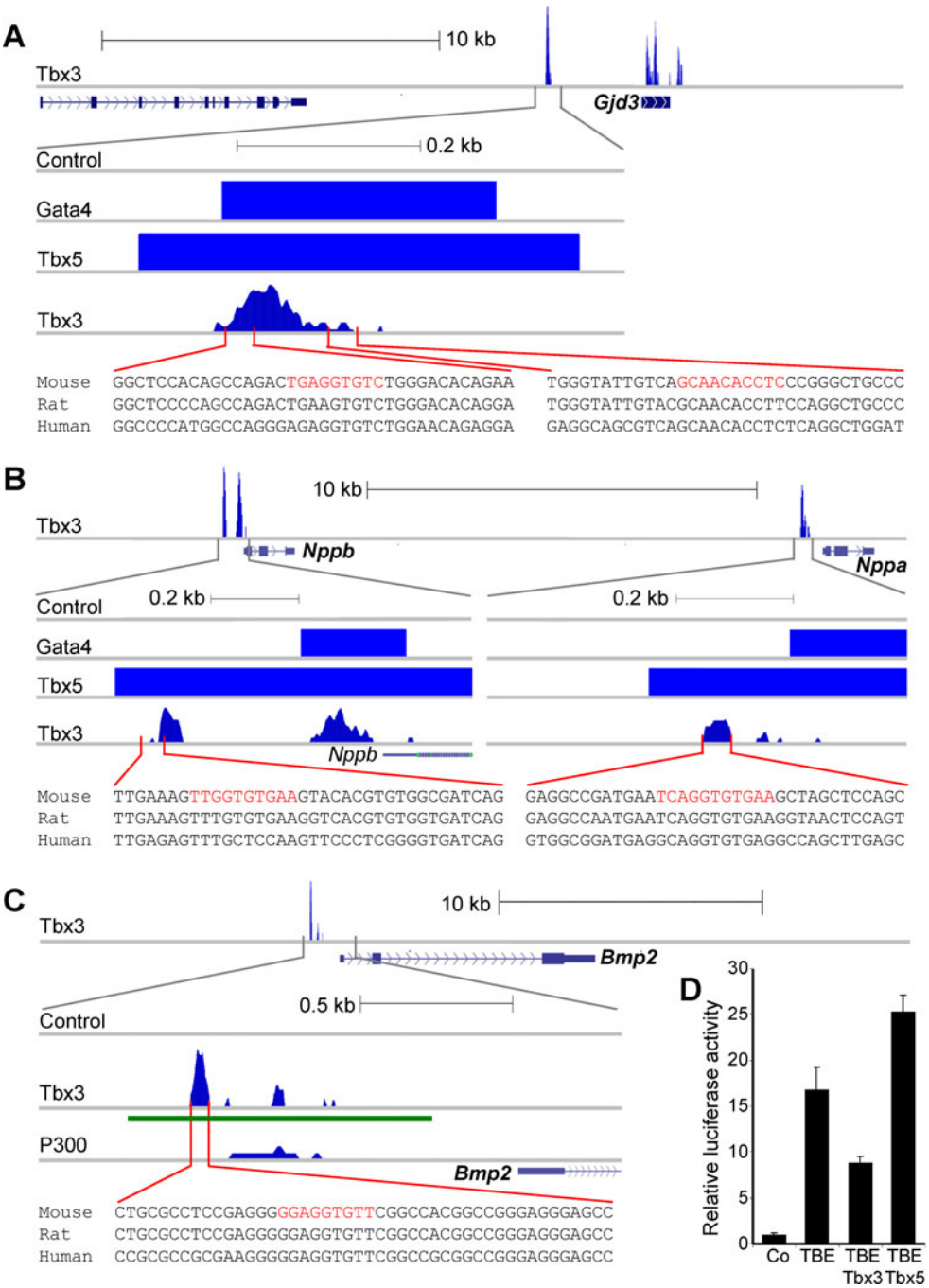

Fig. 6 Tbx3 ChIP-seq reveals interaction with known and novel binding sites in vivo. **a** Tbx3 binds to the region upstream of *Cx30.2* (*Gjd3*), a region shown to function as a T-box responsive enhancer [44]. The relative position and sequence of the published T-box binding elements and conservation are shown at the *bottom* of the *panel* (*red*). Recently published Gata4 and Tbx5 ChIP-seq data from HL-1 cells [46] also shows specific binding within this region. **b** The TBE of *Nppa* [42, 43], is occupied by Tbx3 in atria and by Tbx5 and Gata4 in the HL-1 cell line [46]. Tbx3, Tbx5 and Gata4 binding peaks can also be observed upstream of *Nppb,* a gene showing a similar expression profile and response to Tbx3. **c** Tbx3 binding peaks surrounding the *Bmp2* gene. The upstream element, shown to bind both Tbx3 and P300 [47], was cloned (underlined in *green*) upstream of a minimal promoter driving luciferase. Putative T-binding sequence is shown at the *bottom* of the *panel*. **d** Luciferase induction in H10 cells, relative to the minimal promoter only (Co), by the putative enhancer (TBE) described in **c**. The activity of this element can be modulated by the presence of Tbx3 and Tbx5

data suggest that *Bmp2* may be directly regulated by T-box factors including Tbx3 in the myocardium.

Discussion

Tbx2 and Tbx3 regulate chamber versus AVC development

Our study reveals that the T-box transcription factor Tbx2 together with Tbx3 locally repress chamber differentiation, stimulate development of the AVC myocardium and AV nodal phenotype, and induce AV cushion development, providing a mechanism for the co-localization and coordination of these important processes in heart development.

Tbx2 and Tbx3 are an evolutionary closely related pair of T-box proteins that share identical biochemical properties and are co-expressed in the AVC (reviewed in [48]). Hence, *Tbx2* and *Tbx3* may be functionally redundant in their requirement for AVC establishment. Our data confirmed this hypothesis. Individual loss of function of either *Tbx2* or *Tbx3* did not have a major impact on AVC

development (Fig. 1) [10, 11, 14, 49, 50]. However, *Tbx2/3* double mutant embryos largely failed to establish a morphological AVC. Noteworthy, the Cre inserts in the *Tbx2* and *Tbx3* loci are expressed in the putative AVC region of double mutants, indicating that the upstream regulatory pathway for AVC localized *Tbx2/3* activation (most likely involving Bmp2) has been active. Bmp2 in the AVC myocardium induces *Tbx2* through Smads in vivo [3, 7, 8], and was also required for *Tbx3* expression (Fig. 3a). Both Tbx2 and Tbx3, in turn, were found to be required and sufficient to maintain expression of *Bmp2*. These findings indicate that a feed-forward loop activates and maintains Bmp2 and Tbx2/3 expression, respectively, in the AVC. We anticipate the presence of at least one more layer of regulation for AVC localized expression upstream of *Bmp2*, as *Bmp2* (lacking exon 3) expression itself in the *Bmp2* conditional KO is localized in the putative AVC region (Fig. 3) [3, 7, 8]. The redundancy of the paralogous T-box factor genes is limited to sites of co-expression. In the AVC, *Tbx2* is expressed in a slightly broader and left-sided dominant manner, and indeed, *Tbx2* mutants display a left-sided AVC malformation that functions as an accessory pathway causing ventricular pre-excitation [12]. *Tbx3* expression is unique in the sinus node and AV bundle, which are severely affected in *Tbx3* mutants [1]. Moreover, expression of *Tbx3* is maintained in the AVC, unlike *Tbx2* and *Bmp2*, and may be responsible for the maintenance of the pacemaker-like tissue of the AV conduction system. The double dose of the redundant T-box factors in the AVC may serve to firmly establish the AVC phenotype during early stages of cardiogenesis.

Gain-of-function scenarios revealed that both Tbx2 and Tbx3 are able to suppress expression of specific chamber marker genes and differentiation [13, 26, 51, 52]. Using expression profiling, we now identified of a broad spectrum of working myocardium associated genes, including sarcomere components and mitochondrial genes, suppressed by Tbx3, and induction of genes associated with the pacemaker/conduction system in the atrial working myocardium. These programs underlie the typical phenotype of AVC/conduction system myocardium [1], suggesting that Tbx3 to a large degree is responsible for this pacemaker phenotype. The ChIP-seq analysis identified binding sites of Tbx3 in genes both up- and down-regulated by Tbx3 in myocardium, implying that Tbx3 directly regulates these genes in vivo. Both Tbx2 and Tbx3 have context-dependent repression and activation domains, and can interact with multiple co-factors that may provide repression or activation activities to the protein complex [53]. The regulatory DNA regions that control expression of *Bmp2* and other genes in the heart in vivo have not been established [54]. Whether the T-box factor-sensitive enhancer we identified regulates cardiac *Bmp2* expression in vivo remains to be established.

Tbx2 and Tbx3 induce AV cushion development

Embryos with less than two alleles of *Tbx2/Tbx3* failed to establish AV cushions, which are the precursors of the valves, and contribute to the septal structures and to the fibrous insulation. Conversely, ectopic expression of either Tbx2 or Tbx3 in the myocardium of the developing heart caused the initiation of cushion formation. These observations revealed that Tbx2 and Tbx3 in the AVC are redundantly required and sufficient to initiate cushion formation in the AVC. The mechanism of cushion formation has been extensively studied, and important roles for ligands and receptors of the Tgf-β-superfamily have been exposed [2]. Bmp2 expression in the AVC myocardium is both required and sufficient to induce cushion formation [3, 6, 7]. It activates *Notch1*, *Twist1* and *Tgfb2* in the endocardium, which subsequently regulate *Snai1,2* and EMT [2, 4]. A previous report implicated Tbx2 in the direct activation of *Tgfb2* and *Has2* in myocardium, which subsequently induce cardiac jelly formation and cushion development. In that report, Tbx2 did not induce *Bmp2* or *Bmp4* [9]. Our data do not confirm this model, and indicate a different mechanism. Inactivation of *Tbx2/3* caused loss of *Bmp2* expression and vice versa, Tbx2 and Tbx3 in myocardium directly activate *Bmp2* (and *Bmp4*). Further, inactivation of *Tbx2/3* and of *Bmp2* resulted in very similar phenotypes, which included failed AV cushion development and loss of expression of *Tgfb2* and *Has2*. These data indicate that Tbx2/3 and Bmp2 expression are interdependent and part of the same regulatory network for AVC development. Furthermore, Tgfb2, Has2 and other critical components in the regulation of cushion development (e.g., Notch1, Snai1)[2–4] were activated indirectly and selectively in the endocardium by myocardial Tbx2/3. Consistently, our ChIP-seq data indicated that Tbx3 does not interact with the putative TBEs in *Has2* or *Tgfb2* [9], although the latter contain multiple other sites of Tbx3 interaction (Supplemental Fig. 7). Thus, endocardial activation by Tbx2/3 occurs via Bmp2 or another paracrine signal. Together, our data indicate a mechanism in which Tbx2/3 and Bmp2 maintain expression of each other in a feed-forward loop, and provide evidence that Bmp2 induces expression of genes involved in cushion development and EMT in the endocardium.

Acknowledgments We thank Vincent Wakker, L.Y. Elaine Wong, and Corrie de Gier-de Vries for their contributions and advice. This work was supported by grants from The Netherlands Organization for Scientific Research (Vidi Grant 864.05.006 to V.M.C.; Mozaïek grant NWO-017.004.040 to M.S.R.); the European Community's Seventh Framework Programme contract ('CardioGeNet' 223463 to V.M.C.) and the German Research Foundation for the Cluster of Excellence REBIRTH (from Regenerative Biology of Reconstructive Therapy) at Hannover Medical School (A.K.).

References

1. Christoffels VM, Smits GJ, Kispert A, Moorman AF (2010) Development of the pacemaker tissues of the heart. Circ Res 106:240–254
2. Combs MD, Yutzey KE (2009) Heart valve development: regulatory networks in development and disease. Circ Res 105:408–421
3. Ma L, Lu MF, Schwartz RJ, Martin JF (2005) Bmp2 is essential for cardiac cushion epithelial–mesenchymal transition and myocardial patterning. Development 132:5601–5611
4. Luna-Zurita L, Prados B, Grego-Bessa J, Luxan G, Del MG, Benguria A, Adams RH, Perez-Pomares JM, de la Pompa JL (2010) Integration of a notch-dependent mesenchymal gene program and Bmp2-driven cell invasiveness regulates murine cardiac valve formation. J Clin Invest 120:3493–3507
5. Walsh EP (2007) Interventional electrophysiology in patients with congenital heart disease. Circulation 115:3224–3234
6. Sugi Y, Yamamura H, Okagawa H, Markwald RR (2004) Bone morphogenetic protein-2 can mediate myocardial regulation of atrioventricular cushion mesenchymal cell formation in mice. Dev Biol 269:505–518
7. Yamada M, Revelli JP, Eichele G, Barron M, Schwartz RJ (2000) Expression of chick Tbx-2, Tbx-3, and Tbx-5 genes during early heart development: evidence for BMP2 induction of Tbx2. Dev Biol 228:95–105
8. Singh R, Horsthuis T, Farin HF, Grieskamp T, Norden J, Petry M, Wakker V, Moorman AF, Christoffels VM, Kispert A (2009) Tbx20 interacts with smads to confine tbx2 expression to the atrioventricular canal. Circ Res 105:442–452
9. Shirai M, Imanaka-Yoshida K, Schneider MD, Schwartz RJ, Morisaki T (2009) T-box 2, a mediator of Bmp–Smad signaling, induced hyaluronan synthase 2 and Tgf-beta2 expression and endocardial cushion formation. Proc Natl Acad Sci USA 106:18604–18609
10. Aanhaanen WT, Brons JF, Dominguez JN, Rana MS, Norden J, Airik R, Wakker V, de Gier-de Vries C, Brown NA, Kispert A, Moorman AF, Christoffels VM (2009) The $Tbx2^{+}$ primary myocardium of the atrioventricular canal forms the atrioventricular node and the base of the left ventricle. Circ Res 104(11):1267–1274
11. Harrelson Z, Kelly RG, Goldin SN, Gibson-Brown JJ, Bollag RJ, Silver LM, Papaioannou VE (2004) Tbx2 is essential for patterning the atrioventricular canal and for morphogenesis of the outflow tract during heart development. Development 131:5041–5052
12. Aanhaanen WT, Boukens BJ, Sizarov A, Wakker V, de Gier-de Vries C, van Ginneken AC, Moorman AF, Coronel R, Christoffels VM (2011) Defective Tbx2-dependent patterning of the atrioventricular canal myocardium causes accessory pathway formation in mice. J Clin Invest 121:534–544
13. Hoogaars WM, Engel A, Brons JF, Verkerk AO, de Lange FJ, Wong LY, Bakker ML, Clout DE, Wakker V, Barnett P, Ravesloot JH, Moorman AF, Verheijck EE, Christoffels VM (2007) Tbx3 controls the sinoatrial node gene program and imposes pacemaker function on the atria. Genes Dev 21:1098–1112
14. Bakker ML, Boukens BJ, Mommersteeg MTM, Brons JF, Wakker V, Moorman AFM, Christoffels VM (2008) Transcription factor Tbx3 is required for the specification of the atrioventricular conduction system. Circ Res 102:1340–1349
15. de Lange FJ, Moorman AFM, Christoffels VM (2003) Atrial cardiomyocyte-specific expression of Cre recombinase driven by an Nppa gene fragment. Genesis 37:1–4
16. Agah R, Frenkel PA, French BA, Michael LH, Overbeek PA, Schneider MD (1997) Gene recombination in post-mitotic cells. Targeted expression of Cre recombinase provokes cardiac-restricted, site-specific rearrangement in adult ventricular muscle in vivo. J Clin Invest 100:169–179
17. Sohal DS, Nghiem M, Crackower MA, Witt SA, Kimball TR, Tymitz KM, Penninger JM, Molkentin JD (2001) Temporally regulated and tissue-specific gene manipulations in the adult and embryonic heart using a tamoxifen-inducible Cre protein. Circ Res 89:20–25
18. Luche H, Weber O, Nageswara RT, Blum C, Fehling HJ (2007) Faithful activation of an extra-bright red fluorescent protein in "knock-in" Cre-reporter mice ideally suited for lineage tracing studies. Eur J Immunol 37:43–53
19. Lingbeek ME, Jacobs JJ, van Lohuizen M (2002) The T-box repressors TBX2 and TBX3 specifically regulate the tumor suppressor gene p14ARF via a variant T-site in the initiator. J Biol Chem 277:26120–26127
20. Huber W, von Heydebreck A, Sultmann H, Poustka A, Vingron M (2002) Variance stabilization applied to microarray data calibration and to the quantification of differential expression. Bioinformatics 18(Suppl 1):S96–S104
21. 21 Smyth GK (2004) Linear models and empirical bayes methods for assessing differential expression in microarray experiments. Stat Appl Genet Mol Biol 3**:** Article3
22. Reiner A, Yekutieli D, Benjamini Y (2003) Identifying differentially expressed genes using false discovery rate controlling procedures. Bioinformatics 19:368–375
23. Goeman JJ, van de Geer SA, de Kort F, van Houwelingen HC (2004) A global test for groups of genes: testing association with a clinical outcome. Bioinformatics 20:93–99
24. Ruijter JM, Ramakers C, Hoogaars WM, Karlen Y, Bakker O, van den Hoff MJ, Moorman AF (2009) Amplification efficiency: linking baseline and bias in the analysis of quantitative PCR data. Nucleic Acids Res 37(6):e45
25. Moorman AFM, Houweling AC, de Boer PAJ, Christoffels VM (2001) Sensitive nonradioactive detection of mRNA in tissue sections: novel application of the whole-mount in situ hybridization protocol. J Histochem Cytochem 49:1–8
26. Christoffels VM, Hoogaars WMH, Tessari A, Clout DEW, Moorman AFM, Campione M (2004) T-box transcription factor Tbx2 represses differentiation and formation of the cardiac chambers. Dev Dyn 229:763–770
27. Zirzow S, Ludtke TH, Brons JF, Petry M, Christoffels VM, Kispert A (2009) Expression and requirement of T-box transcription factors Tbx2 and Tbx3 during secondary palate development in the mouse. Dev Biol 336:145–155
28. Camenisch TD, Spicer AP, Brehm-Gibson T, Biesterfeldt J, Augustine ML, Calabro A Jr, Kubalak S, Klewer SE, McDonald JA (2000) Disruption of hyaluronan synthase-2 abrogates normal cardiac morphogenesis and hyaluronan-mediated transformation of epithelium to mesenchyme. J Clin Invest 106:349–360
29. Stypmann J, Engelen MA, Orwat S, Bilbilis K, Rothenburger M, Eckardt L, Haverkamp W, Horst J, Dworniczak B, Pennekamp P (2006) Cardiovascular characterization of Pkd2(+/LacZ) mice, an animal model for the autosomal dominant polycystic kidney disease type 2 (ADPKD2). Int J Cardiol 120:158–166
30. 30 Jelier R, Schuemie MJ, Veldhoven A, Dorssers LC, Jenster G, Kors JA (2008) Anni 2.0: a multipurpose text-mining tool for the life sciences. Genome Biol 9**:**R96

31. Baxter RM, Crowell TP, George JA, Getman ME, Gardner H (2007) The plant pathogenesis related protein GLIPR-2 is highly expressed in fibrotic kidney and promotes epithelial to mesenchymal transition in vitro. Matrix Biol 26:20–29
32. Hellman NE, Spector J, Robinson J, Zuo X, Saunier S, Antignac C, Tobias JW, Lipschutz JH (2008) Matrix metalloproteinase 13 (MMP13) and tissue inhibitor of matrix metalloproteinase 1 (TIMP1), regulated by the MAPK pathway, are both necessary for Madin–Darby canine kidney tubulogenesis. J Biol Chem 283:4272–4282
33. Grotegut S, Von SD, Christofori G, Lehembre F (2006) Hepatocyte growth factor induces cell scattering through MAPK/Egr-1-mediated upregulation of Snail. EMBO J 25:3534–3545
34. Wessels A, Vermeulen JLM, Virágh Sz, Kálmán F, Morris GE, Man NT, Lamers WH, Moorman AFM (1990) Spatial distribution of "tissue-specific" antigens in the developing human heart and skeletal muscle. I. An immunohistochemical analysis of creatine kinase isoenzyme expression patterns. Anat Rec 228: 163–176
35. Houweling AC, Somi S, Massink MPG, Groenen MA, Moorman AFM, Christoffels VM (2005) Comparative analysis of the natriuretic peptide precursor gene cluster in vertebrates reveals loss of ANF and retention of CNP-3 in chicken. Dev Dyn 233: 1076–1082
36. Clouthier DE, Hosoda K, Richardson JA, Williams SC, Yanagisawa H, Kuwaki T, Kumada M, Hammer RE, Yanagisawa M (1998) Cranial and cardiac neural crest defects in endothelin-A receptor-deficient mice. Development 125:813–824
37. Chen H, Shi S, Acosta L, Li W, Lu J, Bao S, Chen Z, Yang Z, Schneider MD, Chien KR, Conway SJ, Yoder MC, Haneline LS, Franco D, Shou W (2004) BMP10 is essential for maintaining cardiac growth during murine cardiogenesis. Development 131:2219–2231
38. Moskowitz IP, Kim JB, Moore ML, Wolf CM, Peterson MA, Shendure J, Nobrega MA, Yokota Y, Berul C, Izumo S, Seidman JG, Seidman CE (2007) A molecular pathway including id2, tbx5, and nkx2–5 required for cardiac conduction system development. Cell 129:1365–1376
39. Stroud DM, Darrow BJ, Kim SD, Zhang J, Jongbloed MRM, Rentschler S, Moskowitz IPG, Seidman J, Fishman GI (2007) Complex genomic rearrangement in CCS-LacZ transgenic mice. Genesis 45:76–82
40. Mery A, Aimond F, Menard C, Mikoshiba K, Michalak M, Puceat M (2005) Initiation of embryonic cardiac pacemaker activity by inositol 1, 4, 5-trisphosphate-dependent calcium signaling. Mol Biol Cell 16:2414–2423
41. Marionneau C, Couette B, Liu J, Li H, Mangoni ME, Nargeot J, Lei M, Escande D, Demolombe S (2005) Specific pattern of ionic channel gene expression associated with pacemaker activity in the mouse heart. J Physiol 562:223–234
42. Habets PEMH, Moorman AFM, Clout DEW, van Roon MA, Lingbeek M, Lohuizen M, Campione M, Christoffels VM (2002) Cooperative action of Tbx2 and Nkx2.5 inhibits ANF expression in the atrioventricular canal: implications for cardiac chamber formation. Genes Dev 16:1234–1246
43. Bruneau BG, Nemer G, Schmitt JP, Charron F, Robitaille L, Caron S, Conner DA, Gessler M, Nemer M, Seidman CE, Seidman JG (2001) A murine model of Holt-Oram syndrome defines roles of the T-box transcription factor Tbx5 in cardiogenesis and disease. Cell 106:709–721
44. Munshi NV, McAnally J, Bezprozvannaya S, Berry JM, Richardson JA, Hill JA, Olson EN (2009) Cx30.2 enhancer analysis identifies Gata4 as a novel regulator of atrioventricular delay. Development 136:2665–2674
45. Ghosh TK, Song FF, Packham EA, Buxton S, Robinson TE, Ronksley J, Self T, Bonser AJ, Brook JD (2009) Physical interaction between TBX5 and MEF2C is required for early heart development. Mol Cell Biol 29:2205–2218
46. He A, Kong SW, Ma Q, Pu WT (2011) Co-occupancy by multiple cardiac transcription factors identifies transcriptional enhancers active in heart. Proc Natl Acad Sci USA 108(14): 5632–5637
47. Blow MJ, McCulley DJ, Li Z, Zhang T, Akiyama JA, Holt A, Plajzer-Frick I, Shoukry M, Wright C, Chen F, Afzal V, Bristow J, Ren B, Black BL, Rubin E.M, Visel A, Pennacchio LA (2010) ChIP-seq identification of weakly conserved heart enhancers. Nat Genet 42:806–810
48. Naiche LA, Harrelson Z, Kelly RG, Papaioannou VE (2005) T-Box genes in vertebrate development. Annu Rev Genet 39:219–239
49. 49 Ribeiro I, Kawakami Y, Buscher D, Raya A, Rodriguez-Leon J, Morita M, Rodriguez Esteban C, Izpisua Belmonte JC (2007) Tbx2 and Tbx3 regulate the dynamics of cell proliferation during heart remodeling. PLoS ONE 2:e398
50. Mesbah K, Harrelson Z, Theveniau-Ruissy M, Papaioannou VE, Kelly RG (2008) Tbx3 is required for outflow tract development. Circ Res 103:743–750
51. Mommersteeg MTM, Hoogaars WMH, Prall OWJ, de Gier-de Vries C, Wiese C, Clout DEW, Papaioannou VE, Brown NA, Harvey RP, Moorman AFM, Christoffels VM (2007) Molecular pathway for the localized formation of the sinoatrial node. Circ Res 100:354–362
52. Dupays L, Kotecha S, Mohun TJ (2009) Tbx2 misexpression impairs deployment of second heart field derived progenitor cells to the arterial pole of the embryonic heart. Dev Biol 333:121–131
53. Butz NV, Campbell CE, Gronostajski RM (2004) Differential target gene activation by TBX2 and TBX2VP16: evidence for activation domain-dependent modulation of gene target specificity. Gene 342:67–76
54. Chandler RL, Chandler KJ, McFarland KA, Mortlock DP (2007) Bmp2 transcription in osteoblast progenitors is regulated by a distant 3′ enhancer located 156.3 kilobases from the promoter. Mol Cell Biol 27:2934–2951